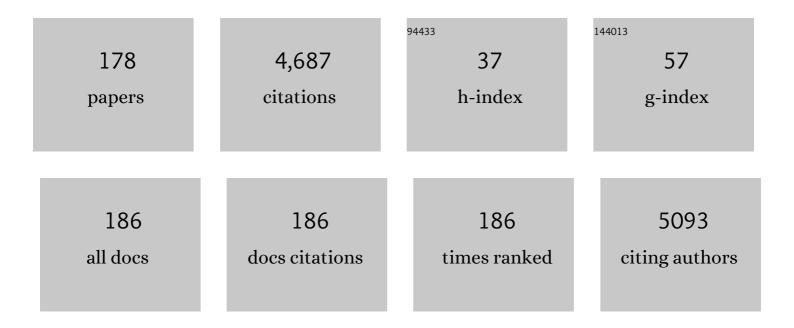
## List of Publications by Year in descending order

Source: https://exaly.com/author-pdf/1339934/publications.pdf Version: 2024-02-01



Нил Сио

#	Article	IF	CITATIONS
1	Reaction Pathway Control via Reactant Vibrational Excitation and Impact on Product Vibrational Distributions: The O + HO <sub>2</sub> → OH + O <sub>2</sub> Atmospheric Reaction. Journal of Physical Chemistry Letters, 2022, 13, 1872-1878.	4.6	4
2	Stereodynamical Control of Cold Collisions of Polyatomic Molecules with Atoms. Journal of Physical Chemistry Letters, 2022, 13, 1777-1784.	4.6	11
3	Semiclassical Trajectory Studies of Reactive and Nonreactive Scattering of OH( <i>A</i> <sup>2</sup> 1£ <sup>+</sup> ) by H <sub>2</sub> Based on an Improved Fullâ€Dimensional Ab Initio Diabatic Potential Energy Matrix. ChemPhysChem, 2022, 23, .	2.1	7
4	Acetylene hydrogenation catalyzed by bare and Ni doped CeO <sub>2</sub> (110): the role of frustrated Lewis pairs. Physical Chemistry Chemical Physics, 2022, 24, 11295-11304.	2.8	12
5	First-Principles Insights into Adiabatic and Nonadiabatic Vibrational Energy-Transfer Dynamics during Molecular Scattering from Metal Surfaces: The Importance of Surface Reactivity. Journal of Physical Chemistry Letters, 2022, 13, 3450-3461.	4.6	9
6	Full-dimensional quantum studies of vibrational energy transfer dynamics between H <sub>2</sub> O and Ar: theory assessing experiment. Physical Chemistry Chemical Physics, 2022, 24, 13542-13549.	2.8	10
7	Mechanism and Dynamics of CO <sub>2</sub> Formation in Formic Acid Decomposition on Pt Surfaces. ACS Catalysis, 2022, 12, 6486-6494.	11.2	2
8	Differential Cross Sections for Cold, State-to-State Spin–Orbit Changing Collisions of NO( <i>v</i> =) Tj ETQq0	0 0 гgBT , 2.5	Oyerlock 10
9	Internal conversion and intersystem crossing dynamics based on coupled potential energy surfaces with full geometry-dependent spinate or bit and derivative couplings. Nonadiabatic photodissociation	2.8	3

	H <sub>2</sub> channel. Physical Chemistry Chemical Physics. 2022. 24. 15060-15067.		
10	Reactive and Nonreactive Collisions between NO(X <sup>2</sup> Î) and O( <sup>3</sup> P) under Hyperthermal Conditions. Journal of Physical Chemistry A, 2022, 126, 4277-4285.	2.5	5
11	Frustrated Lewis Pairs in Heterogeneous Catalysis: Theoretical Insights. Molecules, 2022, 27, 3734.	3.8	5
12	High-fidelity first principles nonadiabaticity: diabatization, analytic representation of global diabatic potential energy matrices, and quantum dynamics. Physical Chemistry Chemical Physics, 2021, 23, 24962-24983.	2.8	29
13	Quasiclassical simulations based on cluster models reveal vibration-facilitated roaming in the isomerization of CO adsorbed on NaCl. Nature Chemistry, 2021, 13, 249-254.	13.6	9
14	Insights into the Formation of Hydroxyl Radicals with Nonthermal Vibrational Excitation in the Meinel Airglow. Journal of Physical Chemistry Letters, 2021, 12, 1822-1828.	4.6	5
15	Insights into adsorption, diffusion, and reactions of atomic nitrogen on a highly oriented pyrolytic graphite surface. Journal of Chemical Physics, 2021, 154, 074708.	3.0	5
16	Single atom catalysis poised to transition from an academic curiosity to an industrially relevant technology. Nature Communications, 2021, 12, 895.	12.8	52
17	Potential energy surfaces for high-energy N + O2 collisions. Journal of Chemical Physics, 2021, 154, 084304.	3.0	23
18	Enabling complete multichannel nonadiabatic dynamics: A global representation of the two-channel coupled, 1,21A and 13A states of NH3 using neural networks. Journal of Chemical Physics, 2021, 154, 094121.	3.0	19

#	Article	IF	CITATIONS
19	Rainbow scattering in rotationally inelastic collisions of HCl and H2. Journal of Chemical Physics, 2021, 154, 104304.	3.0	2
20	Direct Dynamics Simulations of Hyperthermal O(3P) Collisions with Pristine, Defected, Oxygenated, and Nitridated Graphene Surfaces. Journal of Physical Chemistry C, 2021, 125, 9795-9808.	3.1	10
21	Precision test of statistical dynamics with state-to-state ultracold chemistry. Nature, 2021, 593, 379-384.	27.8	53
22	Enabling a Unified Description of Both Internal Conversion and Intersystem Crossing in Formaldehyde: A Global Coupled Quasi-Diabatic Hamiltonian for Its S <sub>0</sub> , S <sub>1</sub> , and T <sub>1</sub> States. Journal of Chemical Theory and Computation, 2021, 17, 4157-4168.	5.3	12
23	Rotational Modulation of Ã2A″-State Photodissociation of HCO via Renner–Teller Nonadiabatic Transitions. Journal of Physical Chemistry Letters, 2021, 12, 6582-6588.	4.6	7
24	Unraveling the Intermediate Reaction Complexes and Critical Role of Support-Derived Oxygen Atoms in CO Oxidation on Single-Atom Pt/CeO <sub>2</sub> . ACS Catalysis, 2021, 11, 8701-8715.	11.2	51
25	Full-Dimensional Global Potential Energy Surface for the KRb + KRb â†' K <sub>2</sub> Rb <sub>2</sub> * â†' K <sub>2</sub> + Rb <sub>2</sub> Reaction with Accurate Long-Range Interactions and Quantum Statistical Calculation of the Product State Distribution under Ultracold Conditions. Journal of Physical Chemistry A. 2021, 125, 6198-6206.	2.5	3
26	Full-dimensional quantum stereodynamics of the non-adiabatic quenching of OH(A2Σ+) by H2. Nature Chemistry, 2021, 13, 909-915.	13.6	17
27	A Time-Independent Quantum Approach to Ro-vibrationally Inelastic Scattering between Atoms and Triatomic Molecules. Journal of Physical Chemistry A, 2021, 125, 6864-6871.	2.5	8
28	Quantum dynamics with ab initio potentials. Journal of Chemical Physics, 2021, 155, 080401.	3.0	2
29	Barium Titanium Oxynitride from Ammonia-Free Nitridation of Reduced BaTiO3. Inorganics, 2021, 9, 62.	2.7	3
30	Dynamics of Initial Hydrogen Spillover from a Single Atom Platinum Active Site to the Cu(111) Host Surface: The Impact of Substrate Electron–Hole Pairs. Journal of Physical Chemistry Letters, 2021, 12, 8423-8429.	4.6	19
31	Vibrational mode-specificity in the dynamics of the Cl + C2H6 → HCl + C2H5 reaction. Journal of Chemical Physics, 2021, 155, 114303.	3.0	14
32	Towards bridging the structure gap in heterogeneous catalysis: the impact of defects in dissociative chemisorption of methane on Ir surfaces. Physical Chemistry Chemical Physics, 2021, 23, 4376-4385.	2.8	31
33	Theoretical H + O <sub>3</sub> rate coefficients from ring polymer molecular dynamics on an accurate global potential energy surface: assessing experimental uncertainties. Physical Chemistry Chemical Physics, 2021, 23, 3300-3310.	2.8	4
34	lsomer-specific kinetics of the C <sup>+</sup> + H <sub>2</sub> O reaction at the temperature of interstellar clouds. Science Advances, 2021, 7, .	10.3	16
35	Vibrational energy pooling <i>via</i> collisions between asymmetric stretching excited CO <sub>2</sub> : a quasi-classical trajectory study on an accurate full-dimensional potential energy surface. Physical Chemistry Chemical Physics, 2021, 23, 24165-24174.	2.8	2
36	Full-Dimensional Potential Energy Surface for Ro-vibrationally Inelastic Scattering between H <sub>2</sub> Molecules. Journal of Chemical Theory and Computation, 2021, 17, 6747-6756.	5.3	11

#	Article	IF	CITATIONS
37	Infrared Activities of Adsorbed Species on Metal Surfaces: The Puzzle of Adsorbed Methyl (CH3). Journal of Physical Chemistry Letters, 2021, 12, 11164-11169.	4.6	0
38	Orbiting resonances in formaldehyde reveal coupling of roaming, radical, and molecular channels. Science, 2021, 374, 1122-1127.	12.6	15
39	Quantum Wave Packet Treatment of Cold Nonadiabatic Reactive Scattering at the State-To-State Level. Journal of Physical Chemistry A, 2021, 125, 10111-10120.	2.5	15
40	Extending the Representation of Multistate Coupled Potential Energy Surfaces To Include Properties Operators Using Neural Networks: Application to the 1,2 <sup>1</sup> A States of Ammonia. Journal of Chemical Theory and Computation, 2020, 16, 302-313.	5.3	39
41	Insights into the Mechanism of Nonadiabatic Photodissociation from Product Vibrational Distributions. The Remarkable Case of Phenol. Journal of Physical Chemistry Letters, 2020, 11, 191-198.	4.6	25
42	Trapping of different stages of BaTiO <sub>3</sub> reduction with LiH. RSC Advances, 2020, 10, 35356-35365.	3.6	5
43	Impact of Diabolical Singular Points on Nonadiabatic Dynamics and a Remedy: Photodissociation of Ammonia in the First Band. Journal of Chemical Theory and Computation, 2020, 16, 6776-6784.	5.3	6
44	Photo-excitation of long-lived transient intermediates in ultracold reactions. Nature Physics, 2020, 16, 1132-1136.	16.7	76
45	Theoretical Investigations of Rate Coefficients for H + O3and HO2+ O Reactions on a Full-Dimensional Potential Energy Surface. Journal of Physical Chemistry A, 2020, 124, 6427-6437.	2.5	16
46	Neural Network Based Quasi-diabatic Representation for S <sub>0</sub> and S <sub>1</sub> States of Formaldehyde. Journal of Physical Chemistry A, 2020, 124, 10132-10142.	2.5	21
47	Exploring reactivity and product formation in N(4S) collisions with pristine and defected graphene with direct dynamics simulations. Journal of Chemical Physics, 2020, 153, 184702.	3.0	13
48	Energy transfer between vibrationally excited carbon monoxide based on a highly accurate six-dimensional potential energy surface. Journal of Chemical Physics, 2020, 153, 054310.	3.0	24
49	Origin of the "odd―behavior in the ultraviolet photochemistry of ozone. Proceedings of the National Academy of Sciences of the United States of America, 2020, 117, 21065-21069.	7.1	10
50	Potential Energy Landscape of CO Adsorbates on NaCl(100) and Implications in Isomerization of Vibrationally Excited CO. Journal of Physical Chemistry C, 2020, 124, 19146-19156.	3.1	12
51	Advances and New Challenges to Bimolecular Reaction Dynamics Theory. Journal of Physical Chemistry Letters, 2020, 11, 8844-8860.	4.6	46
52	Virtual Issue on Combustion Chemistry. Journal of Physical Chemistry A, 2020, 124, 5995-5996.	2.5	0
53	Solid-State NMR Rationalizes the Bone-Adhesive Properties of Serine- and Phosphoserine-Bearing Calcium Phosphate Cements by Unveiling Their Organic/Inorganic Interface. Journal of Physical Chemistry C, 2020, 124, 21512-21531.	3.1	11
54	Spectroscopic identification of the •SSNO isomers. Journal of Chemical Physics, 2020, 153, 094303.	3.0	3

#	Article	IF	CITATIONS
55	Following the microscopic pathway to adsorption through chemisorption and physisorption wells. Science, 2020, 369, 1461-1465.	12.6	42
56	Time-independent quantum theory on vibrational inelastic scattering between atoms and open-shell diatomic molecules: Applications to NO + Ar and NO + H scattering. Journal of Chemical Physics, 2020, 153, 144306.	3.0	13
57	Origin of Confined Catalysis in Nanoscale Reactors between Two-Dimensional Covers and Metal Substrates: Mechanical or Electronic?. Journal of Physical Chemistry C, 2020, 124, 11564-11573.	3.1	14
58	Nonadiabatic Electronic Energy Transfer in the Chemical Oxygen–Iodine Laser: Powered by Derivative Coupling or Spin–Orbit Coupling?. Journal of Physical Chemistry Letters, 2020, 11, 4768-4773.	4.6	10
59	On the nonadiabatic collisional quenching of OH(A) by H <sub>2</sub> : a four coupled quasi-diabatic state description. Physical Chemistry Chemical Physics, 2020, 22, 13516-13527.	2.8	15
60	High-Fidelity Potential Energy Surfaces for Gas-Phase and Gas–Surface Scattering Processes from Machine Learning. Journal of Physical Chemistry Letters, 2020, 11, 5120-5131.	4.6	127
61	A Global Full-Dimensional Potential Energy Surface for the K <sub>2</sub> Rb <sub>2</sub> Complex and Its Lifetime. Journal of Physical Chemistry Letters, 2020, 11, 2605-2610.	4.6	17
62	Characteristics of Impactful Computational Contributions to The Journal of Physical Chemistry A. Journal of Physical Chemistry A, 2020, 124, 5059-5060.	2.5	3
63	Mechanistic Insights into Photocatalyzed H <sub>2</sub> Dissociation on Au Clusters. Journal of the American Chemical Society, 2020, 142, 13090-13101.	13.7	48
64	Many-Body Permutationally Invariant Polynomial Neural Network Potential Energy Surface for N <sub>4</sub> . Journal of Chemical Theory and Computation, 2020, 16, 4822-4832.	5.3	40
65	Statistical quantum mechanical approach to diatom–diatom capture dynamics and application to ultracold KRb + KRb reaction. Journal of Chemical Physics, 2020, 152, 241103.	3.0	19
66	New Perspectives on CO <sub>2</sub> –Pt(111) Interaction with a High-Dimensional Neural Network Potential Energy Surface. Journal of Physical Chemistry C, 2020, 124, 5174-5181.	3.1	37
67	Quantitative phase analyses of biomedical pyrophosphate-bearing monetite and brushite cements by solid-state NMR and powder XRD. Ceramics International, 2020, 46, 11000-11012.	4.8	8
68	Mode Specificity in the OH + HO <sub>2</sub> → H <sub>2</sub> O + O <sub>2</sub> Reaction: Enhancement of Reactivity by Exciting a Spectator Mode. Journal of the American Chemical Society, 2020, 142, 3331-3335.	13.7	33
69	Dissociative Chemisorption of Methane on Stepped Ir(332) Surface: Density Functional Theory and Ab Initio Molecular Dynamics Studies. Journal of Physical Chemistry C, 2019, 123, 20893-20902.	3.1	12
70	Advanced solid-state 1H/31P NMR characterization of pyrophosphate-doped calcium phosphate cements for biomedical applications: The structural role of pyrophosphate. Ceramics International, 2019, 45, 20642-20655.	4.8	22
71	Stereodynamical control of product branching in multi-channel barrierless hydrogen abstraction of CH <sub>3</sub> OH by F. Chemical Science, 2019, 10, 7994-8001.	7.4	24
72	On the mechanism of alkyne hydrogenation catalyzed by Ga-doped ceria. Journal of Catalysis, 2019, 375, 410-418.	6.2	43

#	Article	IF	CITATIONS
73	Globally Accurate Full-Dimensional Potential Energy Surface for H <sub>2</sub> + HCl Inelastic Scattering. Journal of Physical Chemistry A, 2019, 123, 6578-6586.	2.5	10
74	Hot-electron effects during reactive scattering of H <sub>2</sub> from Ag(111): the interplay between mode-specific electronic friction and the potential energy landscape. Chemical Science, 2019, 10, 1089-1097.	7.4	35
75	Hot electron effects during reactive scattering of H <sub>2</sub> from Ag(111): assessing the sensitivity to initial conditions, coupling magnitude, and electronic temperature. Faraday Discussions, 2019, 214, 105-121.	3.2	15
76	Dissection of the multichannel reaction of acetylene with atomic oxygen: from the global potential energy surface to rate coefficients and branching dynamics. Physical Chemistry Chemical Physics, 2019, 21, 1408-1416.	2.8	7
77	Up to a Sign. The Insidious Effects of Energetically Inaccessible Conical Intersections on Unimolecular Reactions. Accounts of Chemical Research, 2019, 52, 501-509.	15.6	39
78	Scattering Dynamics of Glycine, H2O, and CO2 on Highly Oriented Pyrolytic Graphite. Journal of Physical Chemistry C, 2019, 123, 3605-3621.	3.1	7
79	lsotope-selective chemistry in the Be <sup>+</sup> ( <sup>2</sup> S <sub>1/2</sub> ) + HOD → BeOD <sup>+</sup> /BeOH <sup>+</sup> + H/D reaction. Physical Chemistry Chemical Physics, 2019, 21, 14005-14011.	2.8	14
80	First-principles dynamics of collisional intersystem crossing: resonance enhanced quenching of C( <sup>1</sup> D) by N <sub>2</sub> . Physical Chemistry Chemical Physics, 2019, 21, 8645-8653.	2.8	9
81	Competition between Proton Transfer and Proton Isomerization in the N <sub>2</sub> + HOC <sup>+</sup> Reaction on an <i>Ab Initio</i> Based Global Potential Energy Surface. Journal of Physical Chemistry A, 2019, 123, 5347-5355.	2.5	6
82	Neural network based quasi-diabatic Hamiltonians with symmetry adaptation and a correct description of conical intersections. Journal of Chemical Physics, 2019, 150, 214101.	3.0	38
83	Quantum Stereodynamics of H <sub>2</sub> Scattering from Co(0001): Influence of Reaction Channels. Journal of Physical Chemistry C, 2019, 123, 16223-16231.	3.1	8
84	Anab initiobased full-dimensional potential energy surface for OH + O2â‡,, HO3and low-lying vibrational levels of HO3. Physical Chemistry Chemical Physics, 2019, 21, 13766-13775.	2.8	10
85	Photoelectron–Photofragment Coincidence Studies on the Dissociation Dynamics of the OH–CH <sub>4</sub> Complex. Journal of Physical Chemistry A, 2019, 123, 4825-4833.	2.5	8
86	A Quasi-Diabatic Representation of the 1,2 <sup>1</sup> A States of Methylamine. Journal of Physical Chemistry A, 2019, 123, 5231-5241.	2.5	19
87	Au <sub>2</sub> <sup>+</sup> cannot catalyze conversion of methane to ethene at low temperature. Catalysis Science and Technology, 2019, 9, 2767-2780.	4.1	13
88	Dynamics in reactions on metal surfaces: A theoretical perspective. Journal of Chemical Physics, 2019, 150, 180901.	3.0	56
89	Bond dissociation energy of Au2+: A guided ion beam and theoretical investigation. Journal of Chemical Physics, 2019, 150, 174305.	3.0	9
90	Absorption Spectra of Acetylene, Vinylidene, and Their Deuterated Isotopologues on Ab Initio Potential Energy and Dipole Moment Surfaces. Journal of Physical Chemistry A, 2019, 123, 4232-4240.	2.5	7

#	Article	IF	CITATIONS
91	Differential Cross Sections for State-to-State Collisions of NO( <i>v</i> = 10) in Near-Copropagating Beams. Journal of Physical Chemistry Letters, 2019, 10, 2422-2427.	4.6	17
92	Origin of Thermal and Hyperthermal CO <sub>2</sub> from CO Oxidation on Pt Surfaces: The Role of Postâ€Transitionâ€6tate Dynamics, Active Sites, and Chemisorbed CO <sub>2</sub> . Angewandte Chemie, 2019, 131, 6990-6994.	2.0	7
93	Diffraction of CH <sub>4</sub> from a Metal Surface. Journal of Physical Chemistry Letters, 2019, 10, 1574-1580.	4.6	12
94	Origin of Thermal and Hyperthermal CO <sub>2</sub> from CO Oxidation on Pt Surfaces: The Role of Postâ€Transitionâ€State Dynamics, Active Sites, and Chemisorbed CO <sub>2</sub> . Angewandte Chemie - International Edition, 2019, 58, 6916-6920.	13.8	31
95	Accurate characterization of the lowest triplet potential energy surface of SO2 with a coupled cluster method. Journal of Chemical Physics, 2019, 150, 144303.	3.0	2
96	Viewpoint: New Physical Insights from Kinetics Studies. Journal of Physical Chemistry A, 2019, 123, 3057-3057.	2.5	4
97	Steric Effects in CO Oxidation on Pt(111) by Impinging Oxygen Atoms Lead to an Exclusive Hot Atom Mechanism. Journal of Physical Chemistry C, 2019, 123, 10509-10516.	3.1	8
98	Quantum dynamical investigation of product state distributions of the F + CH3OH → HF + CH3O reaction via photodetachment of the F⒒(HOCH3) anion. Journal of Chemical Physics, 2019, 150, 044301.	3.0	5
99	Nonadiabatic Dynamics in Photodissociation of Hydroxymethyl in the 32A(3px) Rydberg State: A Nine-Dimensional Quantum Study. Journal of Physical Chemistry A, 2019, 123, 1937-1944.	2.5	8
100	The Monetite Structure Probed by Advanced Solid-State NMR Experimentation at Fast Magic-Angle Spinning. International Journal of Molecular Sciences, 2019, 20, 6356.	4.1	17
101	Adiabatic and nonadiabatic energy dissipation during scattering of vibrationally excited CO from Au(111). Physical Review B, 2019, 100, .	3.2	23
102	Unexpected Indirect Dynamics in Base-Induced Elimination. Journal of the American Chemical Society, 2019, 141, 20300-20308.	13.7	19
103	Dynamical interference in the vibronic bond breaking reaction of HCO. Science Advances, 2019, 5, eaau0582.	10.3	15
104	Reactive and Nonreactive Scattering of HCl from Au(111): An Ab Initio Molecular Dynamics Study. Journal of Physical Chemistry C, 2019, 123, 2287-2299.	3.1	30
105	Highly Localized SERS Measurements Using Single Silicon Nanowires Decorated with DNA Origami-Based SERS Probe. Nano Letters, 2019, 19, 1061-1066.	9.1	34
106	Representation of coupled adiabatic potential energy surfaces using neural network based quasi-diabatic Hamiltonians: 1,2 <sup>2</sup> A′ states of LiFH. Physical Chemistry Chemical Physics, 2019, 21, 14205-14213.	2.8	45
107	Combined Experimental–Theoretical Study of the OH + CO → H + CO <sub>2</sub> Reaction Dynamics. Journal of Physical Chemistry Letters, 2018, 9, 1229-1236.	4.6	18
108	The near-UV absorber OSSO and its isomers. Chemical Communications, 2018, 54, 4517-4520.	4.1	18

#	Article	IF	CITATIONS
109	Thermal Rate Coefficients and Kinetic Isotope Effects for the Reaction OH + CH <sub>4</sub> → H <sub>2</sub> O + CH <sub>3</sub> on an ab Initio-Based Potential Energy Surface. Journal of Physical Chemistry A, 2018, 122, 2645-2652.	2.5	16
110	First-Principles Insights into Ammonia Decomposition Catalyzed by Ru Clusters Anchored on Carbon Nanotubes: Size Dependence and Interfacial Effects. Journal of Physical Chemistry C, 2018, 122, 9091-9100.	3.1	35
111	Quantum dynamics of ClH2Oâ^' photodetachment: Isotope effect and impact of anion vibrational excitation. Journal of Chemical Physics, 2018, 148, 064305.	3.0	4
112	Machine Learning. Journal of Physical Chemistry A, 2018, 122, 879-879.	2.5	7
113	Autodetachment from Vibrationally Excited Vinylidene Anions. Journal of Physical Chemistry Letters, 2018, 9, 1058-1063.	4.6	15
114	Active vs. spectator modes in nonadiabatic photodissociation dynamics of the hydroxymethyl radical via the 22 <i>A</i> (3 <i>s</i> ) Rydberg state. Journal of Chemical Physics, 2018, 148, 044305.	3.0	11
115	Machine Learning. Journal of Physical Chemistry B, 2018, 122, 1347-1347.	2.6	4
116	Machine Learning. Journal of Physical Chemistry Letters, 2018, 9, 569-569.	4.6	3
117	Signatures of a Conical Intersection in Adiabatic Dissociation on the Ground Electronic State. Journal of the American Chemical Society, 2018, 140, 1986-1989.	13.7	42
118	<i>Ab initio</i> molecular dynamics study of the Eley-Rideal reaction of H + Cl–Au(111) → HCl + Au(111): Impact of energy dissipation to surface phonons and electron-hole pairs. Journal of Chemical Physics, 2018, 148, 014702.	3.0	25
119	Constructing High-Dimensional Neural Network Potential Energy Surfaces for Gas–Surface Scattering and Reactions. Journal of Physical Chemistry C, 2018, 122, 1761-1769.	3.1	78
120	State-to-state mode specificity in H + DOH( $\hat{l}$ /2OH = 1) â†' HD + OH( $\hat{l}$ /22 = 0) reaction: vibrational non-adiabaticity or local-mode excitation?. Physical Chemistry Chemical Physics, 2018, 20, 191-198.	<sup>y</sup> 2.8	12
121	Capture of SO <sub>3</sub> isomers in the oxidation of sulfur monoxide with molecular oxygen. Chemical Communications, 2018, 54, 1690-1693.	4.1	19
122	A Novel Class of Injectable Bioceramics That Glue Tissues and Biomaterials. Materials, 2018, 11, 2492.	2.9	42
123	Modified Gaussian Wave Packet Method for Calculating Initial State Wave Functions in Photodissociation. Journal of Chemical Theory and Computation, 2018, 14, 5527-5534.	5.3	3
124	Permutation invariant polynomial neural network approach to fitting potential energy surfaces. IV. Coupled diabatic potential energy matrices. Journal of Chemical Physics, 2018, 149, 144107.	3.0	61
125	Design of Effective Catalysts for Selective Alkyne Hydrogenation by Doping of Ceria with a Single-Atom Promotor. Journal of the American Chemical Society, 2018, 140, 12964-12973.	13.7	204
126	Correlating DFT Calculations with CO Oxidation Reactivity on Ga-Doped Pt/CeO <sub>2</sub> Single-Atom Catalysts. Journal of Physical Chemistry C, 2018, 122, 22460-22468.	3.1	91

#	Article	IF	CITATIONS
127	Dissociative Chemisorption of O <sub>2</sub> on Al(111): Dynamics on a Correlated Wave-Function-Based Potential Energy Surface. Journal of Physical Chemistry Letters, 2018, 9, 3271-3277.	4.6	40
128	Low temperature rates for key steps of interstellar gas-phase water formation. Science Advances, 2018, 4, eaar3417.	10.3	19
129	Communication: Fingerprints of reaction mechanisms in product distributions: Eley-Rideal-type reactions between D and CD3/Cu(111). Journal of Chemical Physics, 2018, 149, 031101.	3.0	16
130	Stretching vibration is a spectator in nucleophilic substitution. Science Advances, 2018, 4, eaas9544.	10.3	37
131	Influence of Renner–Teller Coupling between Electronic States on H + CO Inelastic Scattering. Journal of Physical Chemistry A, 2018, 122, 6381-6390.	2.5	4
132	Plasmonic Hot-Carrier-Mediated Tunable Photochemical Reactions. ACS Nano, 2018, 12, 8415-8422.	14.6	75
133	Single atom detachment from Cu clusters, and diffusion and trapping on CeO <sub>2</sub> (111): implications in Ostwald ripening and atomic redispersion. Nanoscale, 2018, 10, 17893-17901.	5.6	47
134	Vibrational enhancement in the dynamics of ammonia dissociative chemisorption on Ru(0001). Journal of Chemical Physics, 2018, 149, 044703.	3.0	15
135	Selective hydrogenation of 1,3-butadiene catalyzed by a single Pd atom anchored on graphene: the importance of dynamics. Chemical Science, 2018, 9, 5890-5896.	7.4	55
136	Fermi resonance controlled product branching in the H + HOD reaction. Physical Chemistry Chemical Physics, 2018, 20, 17029-17037.	2.8	16
137	Optical Control of Reactions between Water and Laser-Cooled Be <sup>+</sup> Ions. Journal of Physical Chemistry Letters, 2018, 9, 3555-3560.	4.6	37
138	High-Dimensional Atomistic Neural Network Potentials for Molecule–Surface Interactions: HCl Scattering from Au(111). Journal of Physical Chemistry Letters, 2017, 8, 666-672.	4.6	94
139	Photoabsorption Assignments for the C̃1B2 ↕X̃1A1 Vibronic Transitions of SO2, Using New Ab Initio Potential Energy and Transition Dipole Surfaces. Journal of Physical Chemistry A, 2017, 121, 1012-1021.	2.5	18
140	Ab Initio Molecular Dynamics Study of Dissociative Chemisorption and Scattering of CO <sub>2</sub> on Ni(100): Reactivity, Energy Transfer, Steering Dynamics, and Lattice Effects. Journal of Physical Chemistry C, 2017, 121, 5594-5602.	3.1	41
141	Rotational excitation of the interstellar NH2 radical by H2. Journal of Chemical Physics, 2017, 146, 064309.	3.0	12
142	Adsorption of methylene blue and its N-demethylated derivatives on the (111) face of coinage metals: The importance of dispersion interactions. Journal of Chemical Physics, 2017, 146, 164701.	3.0	17
143	Temperature and Pressure Dependences of the Reactions of Fe <sup>+</sup> with Methyl Halides CH <sub>3</sub> X (X = Cl, Br, I): Experiments and Kinetic Modeling Results. Journal of Physical Chemistry A, 2017, 121, 4058-4068.	2.5	7
144	Final State Resolved Quantum Predissociation Dynamics of SO <sub>2</sub> ( <i>Clƒ</i> <sup>1</sup> <i>B</i> <sub><b>2</b></sub> ) and Its Isotopomers via a Crossing with a Singlet Repulsive State. Journal of Physical Chemistry A, 2017, 121, 4930-4938.	2.5	9

#	Article	IF	CITATIONS
145	First-principles C band absorption spectra of SO <sub>2</sub> and its isotopologues. Journal of Chemical Physics, 2017, 146, 154305.	3.0	7
146	Nonadiabatic photodissociation dynamics of the hydroxymethyl radical via the 22 <i>A</i> (3 <i>s</i> ) Rydberg state: A four-dimensional quantum study. Journal of Chemical Physics, 2017, 146, 224306.	3.0	13
147	Controllable synthesis of LiFePO <sub>4</sub> in different polymorphs and study of the reaction mechanism. Journal of Materials Chemistry A, 2017, 5, 14294-14300.	10.3	25
148	Competition between the H- and D-atom transfer channels in the H <sub>2</sub> O <sup>+</sup> + HD reaction: reduced-dimensional quantum and quasi-classical studies. Physical Chemistry Chemical Physics, 2017, 19, 17396-17403.	2.8	9
149	Constructive and Destructive Interference in Nonadiabatic Tunneling via Conical Intersections. Journal of Chemical Theory and Computation, 2017, 13, 1902-1910.	5.3	34
150	Representing Global Reactive Potential Energy Surfaces Using Gaussian Processes. Journal of Physical Chemistry A, 2017, 121, 2552-2557.	2.5	72
151	Charge Transfer Doping Induced Conformational Ordering of a Non-Crystalline Conjugated Polymer. Journal of Physical Chemistry C, 2017, 121, 23817-23826.	3.1	7
152	Effects of vibrational excitation on the F + H <sub>2</sub> O → HF + OH reaction: dissociative photodetachment of overtone-excited [F–H–OH] <sup>â"</sup> . Chemical Science, 2017, 8, 7821-7833.	7.4	16
153	Encoding of vinylidene isomerization in its anion photoelectron spectrum. Science, 2017, 358, 336-339.	12.6	55
154	Potential energy surface stationary points and dynamics of the F <sup>â^'</sup> + CH <sub>3</sub> I double inversion mechanism. Physical Chemistry Chemical Physics, 2017, 19, 20127-20136.	2.8	31
155	Dynamic mapping of conical intersection seams: A general method for incorporating the geometric phase in adiabatic dynamics in polyatomic systems. Journal of Chemical Physics, 2017, 147, 044109.	3.0	25
156	Excess Li-lon Storage on Reconstructed Surfaces of Nanocrystals To Boost Battery Performance. Nano Letters, 2017, 17, 6018-6026.	9.1	53
157	Kinetics and dynamics of the C( <sup>3</sup> P) + H <sub>2</sub> O reaction on a full-dimensional accurate triplet state potential energy surface. Physical Chemistry Chemical Physics, 2017, 19, 23280-23288.	2.8	13
158	Dynamics of transient species <i>via</i> anion photodetachment. Chemical Society Reviews, 2017, 46, 7650-7667.	38.1	35
159	Dissociative chemisorption of methane on Ni(111) using a chemically accurate fifteen dimensional potential energy surface. Physical Chemistry Chemical Physics, 2017, 19, 30540-30550.	2.8	40
160	Accurate Determination of Tunneling-Affected Rate Coefficients: Theory Assessing Experiment. Journal of Physical Chemistry Letters, 2017, 8, 3392-3397.	4.6	22
161	Surprising behaviors in the temperature dependent kinetics of diatomic interhalogens with anions and cations. Journal of Chemical Physics, 2017, 146, 214307.	3.0	7
162	Considering "Physical Insights―in Theoretical Studies of Gas Phase Processes. Journal of Physical Chemistry A, 2017, 121, 4853-4854.	2.5	1

#	Article	IF	CITATIONS
163	Experimental and theoretical studies of the reactions of ground-state sulfur atoms with hydrogen and deuterium. Journal of Chemical Physics, 2017, 147, 134302.	3.0	6
164	3Dâ€Printed Cathodes of LiMn <sub>1â^'</sub> <i><sub>x</sub></i> Fe <i><sub>x</sub></i> PO <sub>4</sub> Nanocrystals Achieve Both Ultrahigh Rate and High Capacity for Advanced Lithiumâ€ion Battery. Advanced Energy Materials, 2016, 6, 1600856.	19.5	157
165	Optimized Temperature Effect of Liâ€lon Diffusion with Layer Distance in Li(Ni <i><sub>x</sub></i> Mn <i><sub>y</sub></i> Co <i><sub>z</sub></i> )O <sub>2</sub> Cathode Materials for High Performance Liâ€lon Battery. Advanced Energy Materials, 2016, 6, 1501309.	19.5	182
166	On the incorporation of the geometric phase in general single potential energy surface dynamics: A removable approximation to ab initio data. Journal of Chemical Physics, 2016, 145, 234111.	3.0	25
167	The formation and mechanism of nano-monocrystalline γ-Fe <sub>2</sub> O <sub>3</sub> with graphene-shell for high-performance lithium ion batteries. RSC Advances, 2016, 6, 51777-51782.	3.6	12
168	Control of chemical reactivity by transition-state and beyond. Chemical Science, 2016, 7, 3992-4003.	7.4	78
169	Excess lithium storage in LiFePO <sub>4</sub> -Carbon interface by ball-milling. Functional Materials Letters, 2016, 09, 1650053.	1.2	7
170	Non-Adiabatic Effects on Excited States of Vinylidene Observed with Slow Photoelectron Velocity-Map Imaging. Journal of the American Chemical Society, 2016, 138, 16417-16425.	13.7	28
171	Soft-contact conductive carbon enabling depolarization of LiFePO4 cathodes to enhance both capacity and rate performances of lithium ion batteries. Journal of Power Sources, 2016, 331, 232-239.	7.8	41
172	Storage and Effective Migration of Li-lon for Defected β-LiFePO <sub>4</sub> Phase Nanocrystals. Nano Letters, 2016, 16, 601-608.	9.1	31
173	A core–shell nanohollow-γ-Fe <sub>2</sub> O <sub>3</sub> @graphene hybrid prepared through the Kirkendall process as a high performance anode material for lithium ion batteries. Chemical Communications, 2015, 51, 7855-7858.	4.1	76
174	Janus Solid–Liquid Interface Enabling Ultrahigh Charging and Discharging Rate for Advanced Lithium-Ion Batteries. Nano Letters, 2015, 15, 6102-6109.	9.1	90
175	Formation of mono/bi-layer iron phosphate and nucleation of LiFePO 4 nano-crystals from amorphous 2D sheets in charge/discharge process for cathode in high-performance Li-ion batteries. Nano Energy, 2015, 18, 187-195.	16.0	30
176	High sulfur loading composite wrapped by 3D nitrogen-doped graphene as a cathode material for lithium–sulfur batteries. Journal of Materials Chemistry A, 2014, 2, 5018-5023.	10.3	249
177	Unimolecular dissociation dynamics of electronically excited HCO(Ã <sup>2</sup> A′′): rotational control of nonadiabatic decay. Faraday Discussions, 0, 238, 236-248.	3.2	2
178	Representation of Diabatic Potential Energy Matrices for Multiconfiguration Time-Dependent Hartree Treatments of High-Dimensional Nonadiabatic Photodissociation Dynamics. Journal of Chemical Theory and Computation, 0, , .	5.3	1